

Specific and Amplified Voltammetric Detection of Dopamine at Nitrilotriacetic acid-Iron Modified Gold Electrode

Lin Liu*, Guifang Wang, Qingqin Feng, Yun Xing, Hongxing Han, Min Jing,

College of Chemistry and Chemical Engineering, Anyang Normal University, Anyang, Henan, People's Republic of China 455000

*E-mail: liulin@aynu.edu.cn

Received: 22 January 2013 / Accepted: 17 February 2013 / Published: 1 March 2013

Sandwich-type biosensor is one of the major analytical techniques for sensitive and selective detection of biomolecules. In this format, the crucial step is the capture and identification of analytes. In this work, we reported a sandwich-type electrochemical biosensor for the detection of dopamine (DA). Nitrilotriacetic acids complexing Fe(III) were immobilized onto gold electrodes to capture DA. The amino groups of DA were derivatized by biotin for the attachment of gold nanoparticle/streptavidin conjugates capped with multiple ferrocene tags. Well-defined voltammetric peaks of high signal intensity were obtained. DA concentrations ranging from 0.5 to 20 nM can be readily determined. A detection limit of 0.1 nM was achieved, which is lower than those achievable using the modified electrodes reported so far. This method was demonstrated to be highly sensitive, accurate and reproducible.

Keywords: dopamine; gold nanoparticles; voltammetric detection; nitrilotriacetic acid; ferrocene

1. INTRODUCTION

Dopamine (DA) is a monoamine neurotransmitter distributed in the central neural system brain tissues and body fluids of mammals. It plays pivotal roles in the function of central nervous, renal, hormonal and cardiovascular system. Detection and quantification of DA is important in diagnoses, monitoring, prevention and treatments of some certain diseases, such as Parkinson's disease, Alzheimer's disease, Huntington's disease, epilepsy, pheochromocytoma and neuroblastoma [1-4]. DA is an electrochemically active compound. In recent years, the development of voltammetric methods for the determination of DA in human fluid has received considerable interest [5]. However, other biochemical compounds such as uric acid (UA) and ascorbate acid (AA) which levels are 100 ~ 1000 times higher than that of DA are oxidized at nearly same potential. The overlap of their voltammetric

responses makes the sensitive and selective detection highly difficult. To avoid the interference of other biochemical compounds (e.g. AA and UA), various modified electrodes have been constructed [6-14]. Although these electrodes have distinguished the overlap peaks to some extent and achieved the selective or simultaneous determination of DA and other biochemical compounds, the detectable concentration is still higher than that of DA in real sample. Additionally, the oxidation products of DA can react with AA present in sample and regenerate DA that becomes available again for oxidation, which severely limits the accuracy of detection [15]. Therefore, a highly sensitive and selective method is desired for the quantification of DA in the coexistence of other biological species.

Sandwich-type biosensor is one of the major analytical techniques for sensitive and selective detection of biomolecules. In this format, the crucial step is the capture (selectivity) and identification (sensitivity) of analytes [16]. Boronic acids are known to bind with diol compounds containing DA. Various phenylboronic acid-modified electrodes have been constructed for DA detection via the interaction of boronic acid and catechol [15,17-20]. Recently, we, for the first time, reported a sandwich-type electrochemical sensor for the detection of DA. In this system, DA was captured by the boronic acids-covered electrode and then derivatized by biotin for the attachment of ferrocene (Fc)-capped gold nanoparticle/streptavidin (SA-AuNPs) conjugates [18]. However, other members of diol family such as glucose at physiological concentration would interfere in the detection due to the competitive reaction between glucose and DA. Thus, to avoid interference from other biological species, new chips are needed for selective DA capture in the sandwich format.

It has been reported that DA forms stable, robust anchor onto the surface of iron oxide by the interaction of catechol and iron and the amino group of DA makes it easy for the further conjugation of molecules [21-25]. Also, Que et al. found that catechol could form a stable ternary complex with Fe(III) and tetradentate ligands such as nitrilotriacetic acid [26]. Kaya et al. reported that the iron-nitrilotriacetic acid attached silver nanoparticles can selectively capture DA in the presence of excessive ascorbic acid (AA) [27]. Herein, nitrilotriacetic acid-Fe(III)-covered electrodes were employed to capture DA via the interaction of Fe(III) and catechol. The amino group of captured DA reacted then with biotin N-hydroxysuccinimide ester, which facilitated the attachment of Fc-capped SA-AuNPs conjugates. The results indicated that diol derivatives such as glucose and AA at physiological concentration have no interference in the specific detection of DA.

2. EXPERIMENTAL

2.1 Reagents and materials

N - (3 - Dimethylaminopropyl) - *N'* - ethylcarbodiimide hydrochloride (EDC), *N*-hydroxysuccinimide (NHS), 3-mercaptopropionic acid (MPA), biotin N-hydroxysuccinimide ester, 1-hexanethiol (HT), N_{α},N_{α} -bis(carboxymethyl)-L-lysine hydrate (NTA), SA-AuNPs conjugate, 6-ferrocenyl-1-hexanethiol (Fc(CH₂)₆SH), ascorbate acid (AA), adrenaline (Ad), uric acid (UA), tyrosine (Tyr), histidine (His), and 2-amino-2-hydroxymethyl-propane-1,3-diol (Tris) were purchased from Sigma-Aldrich. Dopamine (DA) hydrochloride and noradrenaline (NA) were purchased from Aladdin

Reagent Inc. (China). *N,N*-Dimethylformamide (DMF), ferric nitrate nonahydrate ($\text{Fe}(\text{NO}_3)_3 \cdot 9\text{H}_2\text{O}$), ferrous ammonium sulfate ($\text{Fe}(\text{NH}_4)_2(\text{SO}_4)_2$), propylamine, ethyl acetate, glucose and KClO_4 were of analytical grade and obtained from Beijing Chemical Reagent Co. (Beijing, China). Preparation of the Fc-capped SA-AuPs conjugates followed the reported procedure [28]. Fe(II) solution was prepared freshly by dissolving $\text{Fe}(\text{NH}_4)_2(\text{SO}_4)_2$ in Tris buffer. The stock solution of 10 mM Fe(III) was prepared by dissolving an appropriate amount of $\text{Fe}(\text{NO}_3)_3 \cdot 9\text{H}_2\text{O}$ in 5 mM H_2SO_4 . DA solution was prepared freshly with water and subsequently diluted with Tris buffer to the desired concentrations for assay. All aqueous solutions were prepared with N_2 -saturated deionized water purified by a Millipore system (Simplicity Plus, Millipore Corp.).

Artificial cerebrospinal fluid (ACSF) consisting of 150 mM NaCl, 3 mM KCl, 1.4 mM CaCl_2 , 0.8 mM MgCl_2 , 1 mM phosphate, 0.1 mM AA and 3 mM glucose was prepared in-house. Before assay, the ACSF samples were diluted 20-fold with Tris buffer.

2.2 Instruments

UV-vis spectroscopic measurements were collected on a Cary 50 UV-vis spectrophotometer with a 10 mm quartz spectrophotometer cell. The electrochemical experiments were performed on a CHI 842 electrochemical workstation (CH Instruments) using a homemade plastic electrochemical cell. A gold disk electrode with 2 mm of diameter was used as the working electrodes. The counter and reference electrodes were platinum wire and Ag/AgCl, respectively. Prior to each experiment, the working electrodes were polished with diamond pastes of 15- and 3- μm and alumina pastes of 1- and 0.3- μm in diameter.

2.3 Procedures

A schematic representation of the DA detection via amplified voltammetric oxidation of Fc tags on the SA-AuPs conjugates is illustrated in Fig. 1. The MPA-covered Au electrode was formed by immersing the cleaned substrate in a solution of 10 mM MPA in a dark for 15 hours. Upon formation of the MPA self-assembled monolayers (SAMs), the electrode was removed from the solution. This step was followed by washing the electrode thoroughly with ethanol and water. For NTA immobilization, 20 μL aliquots of the EDC/NHS mixture were cast onto the electrode surface for 20 min. EDC/NHS solution was prepared by mixing 0.2 M EDC with 0.1 M NHS in water right before the MPA film activation step [29, 30]. The activated film was then washed with water and soaked in a 4 mM NTA solution (pH 7.4) for 0.5 h. The NTA coated electrode was performed by cross-linking NTA molecules onto a mixed SAM composed of carboxyl-terminated MPA molecules via the standard amine coupling reaction. Then, 20 μL of 1 M propylamine solution was casted onto the electrode surface for 10 min to block the unreacted sites following by soaking the electrode in an aqueous solution containing 0.1 mM HT for 5 min to block the unreacted gold surface. The electrode was rinsed with absolute ethanol and deionized water. The NTA-Fe(III) film was formed by immersing the electrode in a 10 mM Fe(II) solution for 5 min and then exposing it to air. Notice that Fe(II) instead of

Fe(III) dissolved in N₂-saturated Tris buffer was used here due to the stronger tendency of Fe(III) to hydrolyze to Fe(OH)₃ and/or ferrihydrite gel at neutral pH. After the surface had been carefully rinsed with water, 5 μL of Tris buffer containing a given concentration of analytes was cast onto the electrode surface for 5 min. After the analytes capture step, the electrode was rinsed with water to remove the unattached analytes. To attach the Fc-capped SA-AuNPs conjugate onto the electrode surface covered with analytes, the electrode was first allowed to react with 10 μL of 2 mM biotin N-hydroxysuccinimide ester dissolved in a DMF solution for 15 min. Upon rinsing with a copious amount of water, the electrode was exposed to 10 μL of Fc-capped SA-AuNPs conjugate solution for 30 min. Fc-capped SA-AuNPs conjugates were attached to the biotin surface through the biotin-avidin non-covalent interaction ($K_d = 10^{-15}$ M) [31]. Once the Fc-capped SA-AuNPs was attached onto the electrode surface, the electrode was rinsed with water/ethanol mixture and transferred to a 0.1 M KClO₄ solution and the analytes concentration was determined by scanning the electrode potential within the range of 0.1 – 0.7 V to oxidize the Fc groups on the SA-AuNPs conjugates.

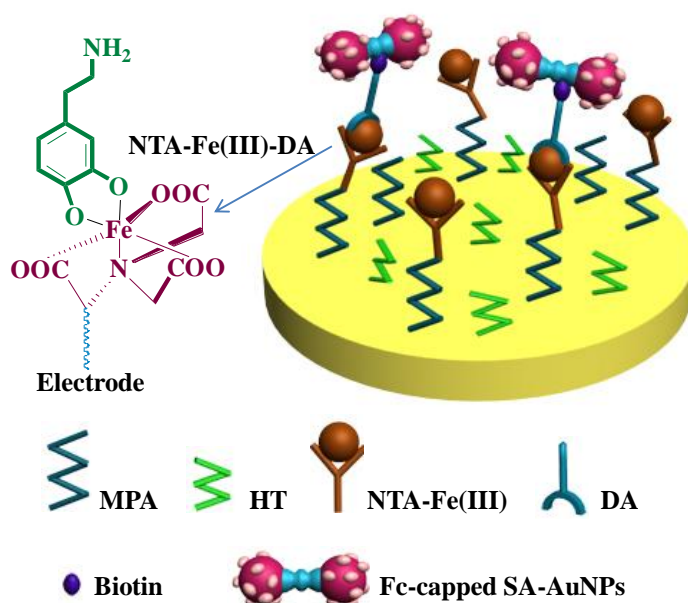


Figure 1. Schematic representation showing the capture of DA by the immobilized NTA–Fe(III) complex and the follow-up Fc-capped gold nanoparticle/streptavidin conjugates attachment.

3. RESULTS AND DISCUSSION

3.1 Formation of the NTA–Fe(III)–DA Ternary Complex

Nitrilotriacetic acid, a tetradentate ligand, is known to form close shell ternary complex with Fe(III) and catechol [26]. The catechol–Fe(III) complex exhibits a characteristic absorption in UV-vis spectrum at around 570 nm corresponding to the phenolate (π) \rightarrow Fe (III) ($d\pi^*$) ligand-to-metal charge transfer (LMCT) transition [32]. Usually a constituent group on the catechol ring or additional ligation to metal center by additional ligand will bring about absorption peak shift. Firstly to validate the formation of ternary complex among DA, Fe(III) and NTA, we measured the UV-vis spectra of

DA/Fe(III) mixture with and without NTA. As shown in Fig. 2. With the ratio of DA/Fe(III) of 2 in the absence of NTA, the characteristic peak at 570 is shown, which is indicative of the formation of the DA–Fe(III) complex. It is generally accepted that at neutral pH Fe(III)(DA)₂ is the dominant form of complexes. With the addition of increased concentration of NTA, the characteristic catecholate-to-Fe(III) LMCT transition absorption peak shifts finally to 615 nm and the peak size decreases remarkably. The shift in the absorption peak position suggests that a new complex involving NTA is formed. The decrease in the peak size suggests that in the complex the DA moiety is decreased, which results in a decreased catecholate-Fe(III) LMCT transition. A point worth to mention is that increasing NTA further than 1 in the ratio of NTA to Fe(III) did not apparently alter the characteristic peak. So the binding affinity of NTA to DA–Fe(III) is estimated to be in the range between the binding affinities of first DA and second DA. The result also demonstrated that NTA replaced the second but not all DA in the Fe(III)(DA)₂ complex.

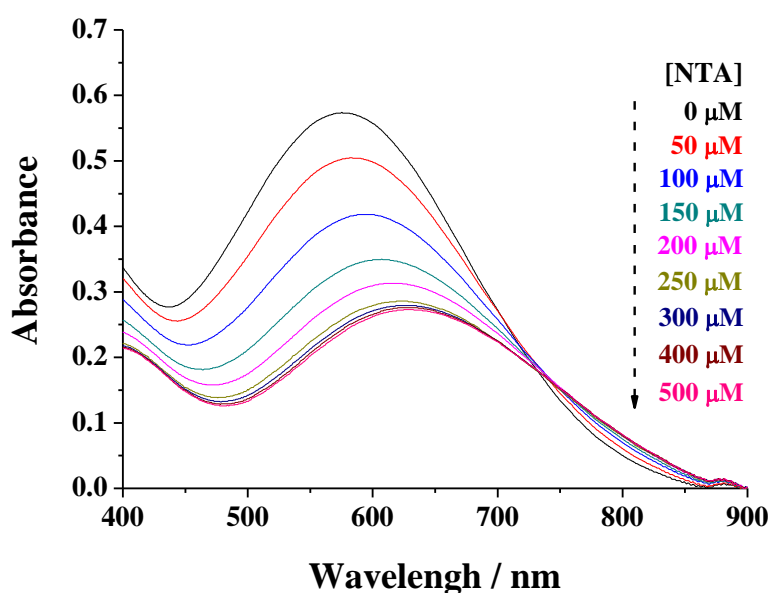


Figure 2. UV-vis absorption DA–Fe(III) and NTA–Fe(III)–DA. The concentrations of DA and Fe(III) were 500 and 250 μM , respectively.

3.2 Determination of DA via amplified cyclic voltammetry

From the above results, two free binding sites of Fe(III) in the NTA–Fe(III) complex are likely to capture DA by the catechol–Fe(III) interaction to form the stable NTA–Fe(III)–DA complex. In the complex, NTA and catechol act as tetradentate and bidentate ligands respectively to yield a distorted octahedral geometry having catechol hydroxides at the axial and equatorial positions [27]. Then, amino group of DA could react with biotin N-hydroxysuccinimide ester, and the Fc-capped SA-AuNPs conjugates were attached to the electrode surface via biotin-streptavidin complexation. Consequently, a facile electron-transfer reaction between the Fc tags and the electrode surface takes place. Previously, Fc-capped SA-AuNPs conjugates have been used to amplified voltammetric detection of protein and

DNA because each gold nanoparticle is capped with a large number of Fc molecules (127 ± 10 Fc molecules) [28]. Thus, the signal intensity will be enhanced remarkably in this sandwich format.

Fig. 3A shows the cyclic voltammograms (CVs) of collected at NTA (green line curve), NTA–Fe(III) (black line curve) and NTA–Fe(III)–DA (red line curve) coated electrodes. In contrast to the CV of the green line curve, the redox waves with $E_{pc} = -0.580$ V and $E_{pa} = 0.105$ V (black line curve) were attributed to the reduction/reoxidation of the iron redox center in the NTA–Fe(III) complex. The irreversibility of the redox peaks is maybe due to the intrinsic property of Fe(III)/Fe(II) in this complex, especially when two sites of iron are occupied by H_2O [33]. After 100 nM DA is coated onto NTA–Fe(III) surface, a small oxidation peak is observed at around 0.5 V (red line curve). Notice that even though the concentration of DA increases to 500 nM, the oxidation current does not change apparently. This indicated that the surface coverage could be saturated by DA. The solid line curve in Fig. 3B is a representative CV collected at an electrode modified with DA followed by biotin coupling and the attachment of the Fc-capped SA-AuNPs conjugates. A pair of well-defined redox waves was obtained. For comparison, the same procedure was implemented with the electrodes without DA modification (green line curve) or biotin coupling (black line curve). The currents in dotted and dashed line curves almost dropped to the background level, indicating that the signal is greatly dependent on DA modification and biotin coupling. The rather small current maybe results from the nonspecific absorption of Fc-capped SA-AuNPs conjugates onto the electrode surface.

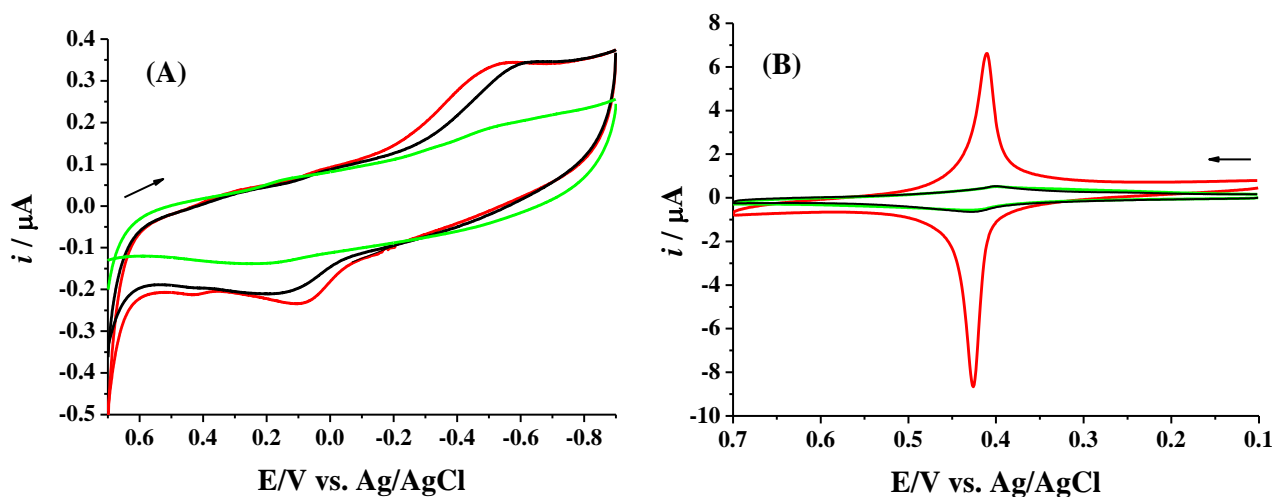


Figure 3. (A) CVs acquired at electrodes covered with NTA (green line curve), NTA–Fe(III) binary complex (black line curve), and NTA–Fe(III)–DA ternary complex (red line curve). (B) CVs at electrodes modified with DA and then Fc-capped SA-AuNPs conjugates (red line curve). The electrochemical responses in the absence of DA (black line curve) or biotin N-hydroxysuccinimide ester (green line curve) followed by the attachment of the conjugates were also shown. The concentration of DA is 100 nM. The scan rate was 0.1 V/s, and the arrow indicates the scan direction.

Previously, it is reported that the tetradentate ligand NTA can form a hexagonal complex with Ni(II) and Cu(II) leaving two binding positions available for binding to a His_6 sequence [31]. These

NTA-metal complexes, especially NTA–Ni(II), have been widely applied to the immobilization of ploy(His)-tagged protein. We also attempted to use the electrodes modified with these complexes to capture DA, but the signal is relatively poor and close to that in the black line curve in Fig 3B. This is understandable since Ni(II) and Cu(II) are all soft metals which exhibits higher binding affinity to N atom of His ($K_d = 1 - 10 \mu\text{M}$) than O atom of catechol. Fe(III) belongs to hard metal. It is suggested that free Fe(III) binds to the first DA with a binding affinity of $4.3 \times 10^{21} \text{M}^{-1}$ and the second DA with that of $2.5 \times 10^{13} \text{M}^{-1}$ [34]. As mentioned above, the binding affinity of NTA to DA–Fe(III) is estimated to be in the range between the binding affinities of first DA and second DA since NTA just replaced the second DA but not all the DA in the Fe(III)(DA)₂ complex. This further indicated that DA was successfully captured by NTA–Fe(III) and the unwanted dissociation of DA or DA–Fe(III) was avoided.

Moreover, we found that reproducible signals can be obtained by immersing the electrode in a 10 mM HCl solution and then rinsing with the water/ethanol mixture to regenerate the surface (i.e., desorbing DA and Fe(III) binding to NTA). After 10 regenerations, there is no apparent decrease in the oxidation current of Fc tags. Therefore, a single NTA coated electrode can be repeatedly used for multiple samples, dramatically decreasing the sample analysis time. Notice that one measurement cycle (modification of DA, assembly of biotin N-hydroxysuccinimide ester, specific absorption of Fc-capped SA-AuNPs conjugates and washing the electrode) takes about 60 min, which is shorter than that of MPA assembly.

3.3 Sensitivity

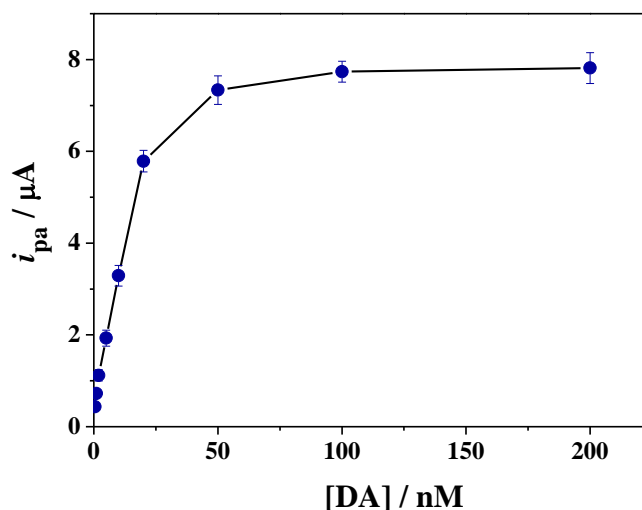


Figure 4. Dependence of the oxidation peak current (i_{pa}) on the concentration of DA. Concentrations of DA determined are 0.5, 1, 2, 5, 10, 20, 50, 100 and 200 nM. Other experimental conditions are the same as those in Fig. 3. The absolute errors were deduced from at least three replicate measurements and are shown as the error bars.

With the regeneration of the method established, we assessed other analytical figures of merit, such as reproducibility, sensitivity and detection limits. The dependence of the oxidation current on the

DA concentration is presented in Fig. 4. The aforementioned regeneration of the sensor surface contributes to the good reproducibility of the method, as the relative standard deviations (RSDs), shown as the error bars in Fig. 4, are all less than 12%. The oxidation current of Fc tags increases sharply within the concentration range of 0.5 – 20 nM but begins to level off beyond 50 nM. The plateau exhibited by the curve is indicative of the attainment of the “saturated” coverage by DA. The current increases linearly with [DA] between 0.5 nM and 20 nM, which can be expressed by $i_{pa} (\mu\text{A}) = 0.281[\text{DA}] (10^{-9} \text{ mol L}^{-1}) + 0.359 (R^2 = 0.995)$. The detection limit (3σ) of the method was estimated to be 0.1 nM. This value is lower than those achievable using the modified electrodes reported so far [6-14]. The lower detection limit is a result of the combined effect of high redox activity of Fc and amplification of Fc-capped AuNPs.

3.4 Selectivity and interference

The selectivity of the present approach was evaluated by testing other biomolecules that coexist in the body fluids of mammals. As a result, we found that no significant oxidation currents were obtained when the NTA–Fe(III)-modified electrodes were incubated in the solution containing each of the interfering agents (black bars in Fig. 5). For AA, glucose, His, Tyr and UA, these results are understandable because they have no benzene with two hydroxyl side groups and cannot adsorb onto the NTA–Fe(III) surface. Although Ad can react with NTA–Fe(III), it has no primary amine groups. Thus, biotin cannot be assembled onto the surface via the amine coupling reaction, making Fc-capped SA-AuNPs conjugates impossible to be captured through the strong biotin-streptavidin interaction. Interestingly, although NA has a similar structure with DA consisting of benzene with two hydroxyl side groups and a side-chain primary amine, it did not induce significant voltammetric signals. We presume that this behavior is caused by its poor reactivity to biotin N-hydroxysuccinimide ester due to the ortho-effect of the hydroxy group [35].

To further investigate the interference, the NTA–Fe(III) modified electrodes were incubated in 10 nM of DA solution containing 100 nM of different interfering agent (blue bars in Fig. 5). Among these amino acids and redox-active biological species, only Ad and NA caused a remarkable decrease in current in comparison with the result obtained in the presence of DA only (red bars). The decrease caused by Ad/NA is maybe due to the competition of affinity between Ad/NA and DA. While Ad/NA modified surface cannot react with biotin N-hydroxysuccinimide ester, making Fc-capped AuNPs impossible to be adsorbed on the electrode surface. Notice that levels of these two catechol compounds *in vivo* are extremely low and comparable to (or even lower than) that of DA (approximately 10 nM) [15,35-38]. We found that these two compounds at a concentration of 10 nM did not cause a significant decrease in the oxidation peak current. Additionally, real samples, such as blood, urine or cerebrospinal fluid, contain micromolar glucose concentrations, over 10^5 times higher than that of DA. We also found that 3 mM glucose did not cause a significant decrease in the oxidation peak current, indicating that NTA–Fe(III) chip has high selectivity to DA.

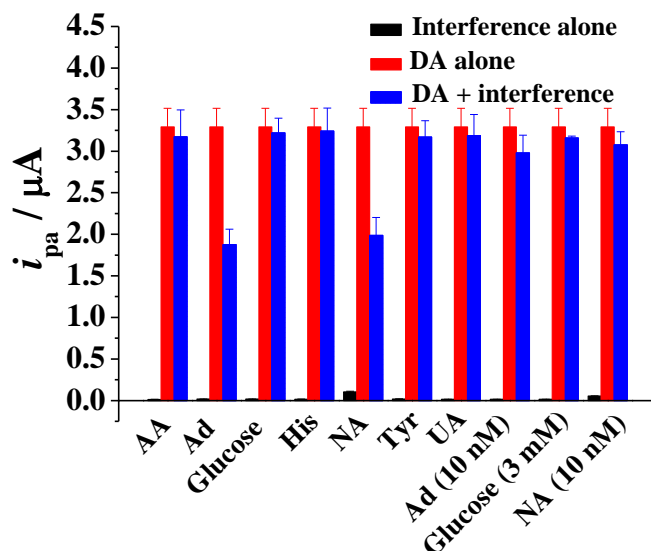


Figure 5. (A) Selectivity and interference of the sensing protocol. The NTA-Fe(III)-modified electrodes were modified with interferences in the absence (black bars) and presence (red and blue bars) of 10 nM DA. Unless otherwise noted, the concentration of interference was 100 nM. Other experimental conditions are the same as those in Fig. 3.

3.5 Artificial sample detection

To demonstrate the viability of the NTA-Fe(III) modified electrodes for amplified voltammetric analysis of real samples, we carried out the measurement of trace amounts of DA in artificial sample prepared as aforementioned procedures. The black line curve in Fig. 6 is the CV collected at the electrode after treatment with artificial sample followed by biotin coupling and attachment of the Fc-capped SA-AuNPs conjugates.

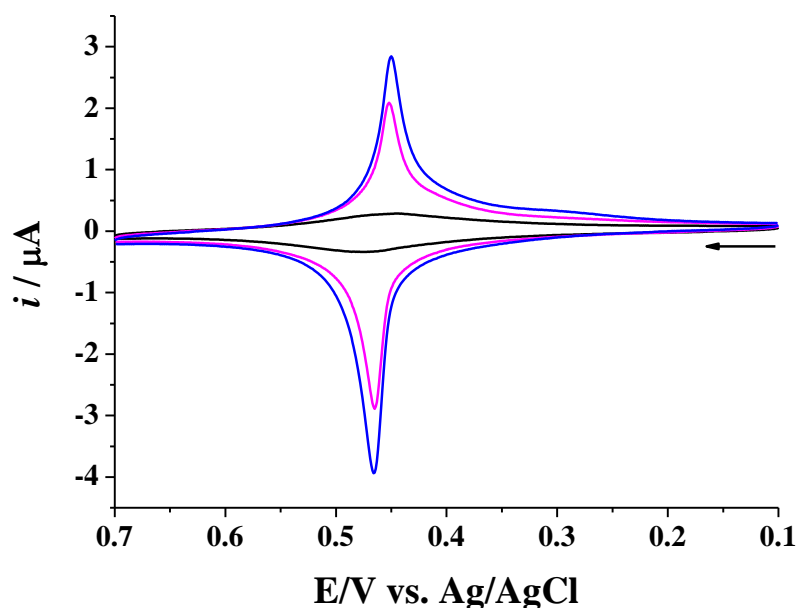


Figure 6. CVs depicting the detection of DA in artificial sample.

The peak current is close to the background level (cf. Fig. 3B) and no DA was found in the sample according to the calibration curve. Then, different concentration of DA was added into the sample and then analyzed. The contents of DA were deduced to be 8.25 nM (magenta line curve) and 12.06 nM (blue line curve) by the calibration curve in Fig. 4, which are closed to the added amounts of 8 nM and 12.5 nM.

4. CONCLUSIONS

In this work, specific binding between DA in solution and NTA-Fe(III) pre-immobilized onto the electrode was used for detecting DA at trace levels. The small number of DA molecules bound to NTA-Fe(III) were tagged with gold nanoparticles capped with a large number of Fc tags. Well-defined Fc voltammetric peaks, whose currents increase with the DA concentration at the surface, were observed. Analytical figures of merit (e.g., dynamic range, reproducibility, selectivity, and detection level) were evaluated through the analysis of different DA concentrations in the presence and absence of other biochemical compounds. The remarkable sensitivity and good selectivity of this method facilitated the measurements of the level of DA present in artificial cerebrospinal fluid sample..

ACKNOWLEDGEMENTS

Partial support of this work by National Natural Science Foundation of China (21205003), the China Scholarship Council (2009637056) and the Graduate Degree Thesis Innovation Foundation of Hunan Province (CX2011B082) is gratefully acknowledged.

References

1. A. H. Liu, I. Honma and H. S. Zhou, *Biosens. Bioelectron.*, 21 (2005) 809.
2. L. Liu, S. Li, L. Liu, D. Deng and N. Xia, *Analyst*, 137 (2012) 3794.
3. M. Tsunoda, *Anal. Bioanal. Chem.*, 386 (2006) 506.
4. R. M. Wightman, L. J. May and A. C. Michael, *Anal Chem*, 60 (1988) 769A.
5. G. P. Jin, X. Peng and Y. F. Ding, *Biosens. Bioelectron.*, 24 (2008) 1031.
6. M. Noroozifar, M. Khorasani-Motlagh, R. Akbari and M. B. Parizi, *Biosens. Bioelectron.*, 28 (2011) 56.
7. C. Wang, R. Yuan, Y. Chai, Y. Zhang, F. Hu and M. Zhang, *Biosens. Bioelectron.*, 30 (2011) 315.
8. A. S. Adekunle, J. G. Ayenimo, X. Y. Fang, W. O. Doherty, O. A. Arotiba and B. B. Mamba, *Int. J. Electrochem. Sci.*, 6 (2011) 2826.
9. N. F. Atta, A. Galal and S. M. Azab, *Int. J. Electrochem. Sci.*, 6 (2011) 5082.
10. A. A. Ensafi, M. Taei and T. Khayamian, *Int. J. Electrochem. Sci.*, 5 (2010) 116.
11. K. C. Lin, C. Y. Yin and S. M. Chen, *Int. J. Electrochem. Sci.*, 6 (2011) 3951.
12. M. Mazloum-Ardakani, H. Rajabi, H. Beitollahi, B. B. F. Mirjalili, A. Akbari and N. Taghavinia, *Int. J. Electrochem. Sci.*, 5 (2010) 147.
13. R. R. Naik, E. Niranjana, B. E. K. Swamy, B. S. Sherigara and H. Jayadevappa, *Int. J. Electrochem. Sci.*, 3 (2008) 1574.
14. H. R. Zare and N. Nasirizadeh, *Int. J. Electrochem. Sci.*, 4 (2009) 1691.
15. S. R. Ali, Y. Ma, R. R. Parajuli, Y. Balogun, W. Y. C. Lai and H. He, *Anal. Chem.*, 79 (2007) 2583.

16. N. Xia, D. Deng, L. Zhang, B. Yuan, M. Jing, J. Du and L. Liu, *Biosens. Bioelectron.*, 43 (2013) 155.
17. B. Fabre and L. Taillebois, *Chem. Commun.* (2003) 2982.
18. L. Liu, J. Du, S. Li, B. Yuan, H. Han, M. Jing and N. Xia, *Biosens. Bioelectron.*, 41 (2013) 730.
19. S. M. Strawbridge, S. J. Green and J. H. R. Tucker, *Chem. Commun.* (2000) 2393.
20. W. Wu, H. Zhu, L. Fan, D. Liu, R. Renneberg and S. Yang, *Chem. Commun.* (2007) 2345.
21. M. D. Shultz, J. U. Reveles, S. N. Khanna and E. E. Carpenter, *J. Am. Chem. Soc.*, 129 (2007) 2482.
22. C. J. Xu, K. M. Xu, H. W. Gu, R. K. Zheng, H. Liu, X. X. Zhang, Z. H. Guo and B. J. Xu, *J. Am. Chem. Soc.*, 126 (2004) 9938.
23. H. W. Gu, Z. M. Yang, J. H. Gao, C. K. Chang and B. Xu, *J. Am. Chem. Soc.*, 127 (2005) 34.
24. B. D. Wang, C. J. Xu, J. Xie, Z. Y. Yang and S. H. Sun, *J. Am. Chem. Soc.*, 130 (2008) 14436.
25. H. Li, Q. Wei, J. He, T. Li, Y. Zhao, Y. Cai, B. Du, Z. Qian and M. Yang, *Biosens. Bioelectron.*, 26 (2011) 3590.
26. L. Que Jr., R. C. Kolanczyk and L. S. White, *J. Am. Chem. Soc.*, 109 (1987) 5373.
27. M. Kaya and M. Volkan, *Anal. Chem.*, 84 (2012) 7729.
28. J. Wang, J. Li, A. J. Baca, J. Hu, F. Zhou, W. Yan and D. Pang, *Anal. Chem.*, 75 (2003) 3941.
29. L. Liu, D. Deng, Y. Xing, S. Li, B. Yuan, J. Chen and N. Xia, *Electrochim. Acta*, 89 (2013) 616.
30. N. Xia, Y. Xing, G. Wang, Q. Feng, Q. Chen, H. Feng, X. Sun and L. Liu, *Int. J. Electrochem. Sci.*, 8 (2013) 1.
31. D. Samanta and A. Sarkar, *Chem. Soc. Rev.*, 40 (2011) 2567.
32. D. Zirong, S. Bhattacharya, J. K. McCusker, P. M. Hagen, D. N. Hendrickson and C. G. Pierpont, *Inorg. Chem.*, 31 (1992) 870.
33. R. L. McCreery, *Chem. Rev.*, 108 (2008) 2646.
34. L. K. Charkoudian and K. J. Franz, *Inorg. Chem.*, 45 (2006) 3657.
35. B. Kong, A. Zhu, Y. Luo, Y. Tian, Y. Yu and G. Shi, *Angew. Chem. Int. Ed.*, 50 (2011) 1837.
36. A. Liu, I. Honma and H. Zhou, *Biosens. Bioelectron.*, 23 (2007) 74.
37. M. Tsunoda, C. Aoyama, S. Ota, T. Tamura and T. Funatsu, *Anal. Methods*, 3 (2011) 582.
38. A. P. Vandas, M. Menenakou, T. H. Kouimitzis and L. Papagiannoulis, *J. Oral Rehabil.*, 26 (1999) 103.